

The Pennsylvania State University

The Graduate School

College of Engineering

**RAPID SILICON CARBIDE CRYSTAL GROWTH WITH HIGH POWER LASER
HEATING METHOD**

A Thesis in

Electrical Engineering

by

Haonan Zhou

© 2017 Haonan Zhou

Submitted in Partial Fulfillment
of the Requirements
for the Degree of

Master of Science

August 2017

The thesis of Haonan Zhou was reviewed and approved* by the following:

Stuart Yin
Professor of Electrical Engineering
Thesis Advisor

Weihua Guan
Assistant Professor of Electrical Engineering

Kultegin Aydin
Professor of Electrical Engineering
Head of the Department of Electronic Engineering

*Signatures are on file in the Graduate School

ABSTRACT

This research presents an ultra-fast procedure to grow silicon carbide crystal with the size up to 50 μm from Nano size powder. By using high power laser beam in vacuum environment, the silicon carbide nanometer powder will be heated to an extremely high temperature in few seconds. The laser beam will be held for several minutes and then cooling down slowly. The silicon carbide powder will grow to micro size crystal in minutes. This research examines the silicon carbide structure before and after the laser beam heating. The composition of the final product is determined by SEM, EDS and XRD. The type of main product and the growing direction is characterized and the growing process presents in two steps. For comparison, different percentages of power and heating methods applied for laser beam.

TABLE OF CONTENTS

List of Figures	v
List of Tables	vi
Acknowledgements.....	vii
Chapter 1 Introduction	1
Introduction of silicon carbide	1
Background of silicon carbide	1
Properties and applications of silicon carbide	1
Chemical properties	2
Physical properties	2
Optical properties	3
Existed methods of growing silicon carbide and their characters	3
Chapter 2 Experimental setup and procedures.....	5
Sample preparation	5
Construction of laser system	6
Experiment conditions	7
Chapter 3 Results and discussion.....	8
Scanning electron microscopy results and discussion	8
Energy dispersive spectroscopy results and discussion	15
X-ray diffraction results and discussion	16
Chapter 4 Conclusion.....	17
Chapter 5 References	18
Appendix A Tables	20
Appendix B Figures	21

LIST OF FIGURES

Figure 1. The setup of the experiment equipment.	6
Figure 2-2. The enlarged view of the chamber.	7
Figure 3-1. Sample heating two minutes with 5% power and cooling immediately after heating.....	8
Figure 3-2. The central area of the sample.....	9
Figure 4-1. Sample heating for two minutes with 12% power and cooling slowly for another two minutes.	10
Figure 4-2. Crystals with clear edge.	10
Figure 4-3. The largest crystal.	11
Figure 4-4. Original powder on surface	11
Figure 5-1. Original surface.....	12
Figure 5-2. Middle layer after heating.	12
Figure 5-3. Microstructures of surface.....	12
Figure 5-2. Microstructures of middle layer.	12
Figure 6-1. The vertical view of the cross section of the heating hole.	13
Figure 6-2. The side view of the cross section.....	14
Figure 7. The energy dispersive spectroscopy result.	15
Figure 8. The X-ray diffraction result.....	16

LIST OF TABLES

Table 1. Prepared samples' weight.....	5
Table 2. Experiment conditions.....	7

ACKNOWLEDGEMENTS

First of all, I would like to take this opportunity to acknowledge Dr. Yin. This thesis would not be possible to finish without his generous guidance. Besides the help in academics, he also plays the role of mentor with full of patient in my life. It was a great pleasure to work with him.

I am highly indebted to the group members: Mr. Chang-Jiang Chen, Mr. Wenbin Zhu and Mr. Jo-Hung Chao for providing me generous help in research. Especially Chang-Jiang, took lots of time helping me with SEM and EDS analysis. And he also gave me advices to improve the experiments.

I wish to express my sincere thanks to Dr. Guan, my committee member, for showing interests in my research and giving his precious advices.

Chapter 1

Introduction

Introduction of silicon carbide

Silicon carbide, as one of the newest generation semiconductors, has multiple advantages in electrical and optical properties including high breakdown voltage, high thermal conductivities and a wide band gap which can be applied in equipment with high temperatures and power (Casady and Johnson, 1996). It has outstanding performance in chemical and physical properties as well. With so many unique properties, silicon carbide must play an important role in high-tech field in the future.

Background of silicon carbide

Silicon carbide is a binary compound in IV family. As they both have four outer layer electrons, silicon and carbon are connected with covalent bonds with the atomic ratio of 1:1, which is very stable and has high hardness and melting point (Hillenbrand *et al.* 2002, Greffet *et al.* 2002). With a similar hexahedral crystal structure of diamond, the hardness can reach to 9.2 to 9.5 in Mohs hardness scales.

One of the most notable features of silicon carbide is the homogenous pleomorphism (Cheung, 2006). The basic structural unit of silicon carbide is tetrahedron consisted with silicon and carbon. They are close packaged which indicates a high strength between these units. The slip barrier between the close packaged plane, however, is extremely low and this causes polymorphs. There

are two main typical structure categories of silicon carbide: one is α -SiC with hexagonal structures and the other type is cubic crystal called β -SiC or 3C-SiC. Among all homogeneous polymorphism, β -SiC has the minimum bond energy and largest lattice free energy (Muranaka *et al.* 2008).

Properties and applications of silicon carbide

Chemical properties

Silicon carbide with high chemical stability can resist most of the acid and alkali corrosion. But the resistance to alkali is weaker than acid. It also has oxidation resistance. Due to its high thermal stability, silicon carbide doesn't react to form silica until the temperature reaches 1300°C in the open air and the silica layer can prevent the internal part from oxidation reaction. In other words, silicon carbide can be used in all kinds of smelting furnace lining, high temperature furnaces artifacts, etc. (Scace and Slack. 1959) Therefore, it can be used as high temperature indirect heating material in non-ferrous metal smelting industry.

Physical properties

Silicon carbide is a high quality refractory material with excellent thermal performance: high thermal conductivity and small thermal expansion coefficient. It also has a good radiation resistance which is 10-100 times larger than silicon. Therefore, silicon carbide devices have a greater ability to against high-energy rays from cosmos, and this makes silicon carbide devices have more advantages than silicon devices in satellite, aerospace and nuclear instrument applications (Ruddy *et al.* 1998). With high acoustic propagation velocity, silicon carbide is also

available for surface acoustic wave devices (Ilyakhinskii *et al.* 2016). Because of the high hardness, silicon carbide also has important use in abrasive area.

Optical properties

As early as in 1923, people have already found that silicon carbide has the injection electroluminescent phenomenon (Kruangam *et al.* 1985). And the reason is that it is an indirect band gap semiconductor material. The indirect composite process between the impurity levels generates the light. By mixing with different impurities, silicon carbide can change the light wavelength and its range covers various colors from red to purple. Emitting Blu-ray has the most important significance. With a short wavelength, blue light can greatly improve optical information storage density. So silicon carbide blue light devices can be applied in underwater information communication.

Existed methods of growing silicon carbide and their characters

Without a specific melting point, silicon carbide is hard to grow. The decomposition effect is also an important difficult to overcome. So far, the most popular method is the sublimation method.

Sublimation recrystallization method has been used to grow silicon carbide crystal wafers. By heating up to 2500°C in a porous graphite tube, silicon carbide sublimates and then condenses to hexagonal single crystal in different sizes inside the graphite cavity. This method cannot provide high quality silicon carbide in great amount (Rastegaev *et al.* 1999)

Two-step synthesis can control the size of the crystal by changing the material formula and synthesis process. The first step is to heat silica and carbon particles to 1600°C for 5-10 hours. The second step is to mix the presintering product and crystal growth substance and heat up to higher than 1900°C for 2-10 hours. With this long-lasting heating time, the cost of this synthesis method is very high (Weaver. 1990)

By heating anthracite with particle size less than 5 μm and silica with particle size less than 1 μm up to 1900°C, Nadkarni's group grew silicon carbide crystals with average diameter of 10-30 μm and thickness of 1-5 μm . Based on Nadkarni's work, Parent's group controlled the crystal size by adding silicon carbide particles. This methods' raw materials can be selected widely and suitable for mass production. But the size of the crystal can't be large enough (Nadkarni et al. 1992, Parent. 1993).

Considering the cost and the output ratio problem, new method should be tested. High temperature laser beam is a good heating source. Since high power laser can reach to thousands of degrees' temperature in seconds, the energy loss will be small and the main cost of the experiment is the cost for the silicon carbide Nano-powder. The decomposition is largely reduced. This is a high efficiency with low cost method to grow silicon carbide crystals.

Chapter 2

Experimental setup and procedures

Sample preparation

Silicon carbide powder with size of 0.2 micrometer has been used in this research. Since powder cannot fit the requirement of this research, silicon carbide pills are made with the diameters of 1.5 centimeters and the thickness of 0.3 centimeters. The table shown below presents each sample pill's weight.

Table 1. Prepared samples' weight.

Number	Weight (g)	Number	Weight (g)
1	0.7001	11	0.6987
2	0.7006	12	0.7035
3	0.6985	13	0.7003
4	0.7013	14	0.7004
5	0.6989	15	0.6994
6	0.7011	16	0.7021
7	0.7012	17	0.6987
8	0.7020	18	0.6998
9	0.7003	19	0.7018
10	0.7015	20	0.7006

Laser system construction

The heating source is carbon dioxide laser, which can emit high power invisible light. All the equipment are set in the proper position shown below in figure 1. To make sure the safety in lab, stabilized HeNe laser, which can emit red beam, is used to help control the invisible laser beam. The middle transparent lens is used for aligning the two laser beams together. Thick bricks are used in the test at the possible light path way to protect other equipment in lab. And before final heating, a focus lens is used for focusing the beam to gain the highest energy.

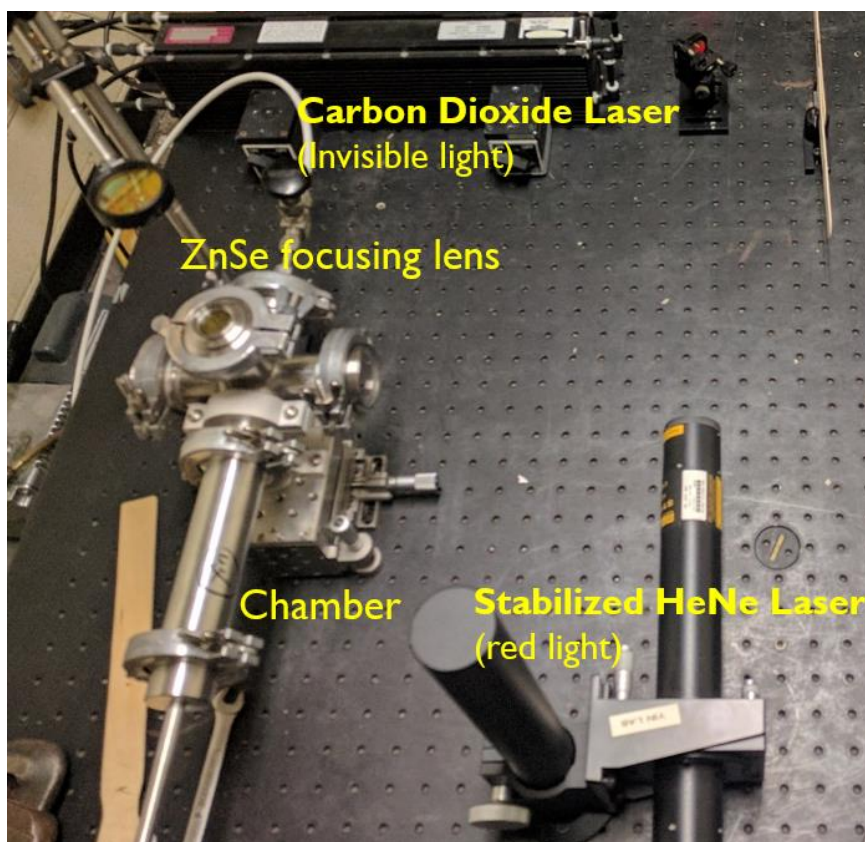


Figure 1. The setup of the experiment equipment.

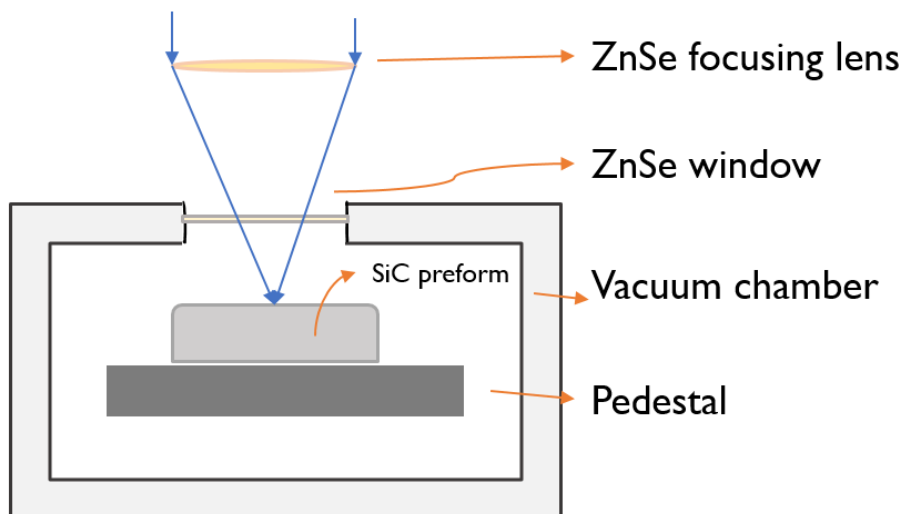


Figure 2. The enlarged view of the chamber.

Experiment conditions

The table 2 presents the experiment settings. The power of the laser was set from 20 to 30 W. The focusing spot size is 1mm^2 . The heating time is from 2 to 3 minutes and the cooling time is 2 minutes.

Table 2. The conditions of experiments.

Settings	Value
Laser power	20-30W
Focusing spot size	1mm^2
Exposure time	2-3min
Cooling time	2min

Chapter 3

The results and discussions

Scanning electron microscopy results and discussion

The figure 3-1 shown below is the sample heating two minutes with 5% power and cooling immediately after heating. From the figure 3-2, some mulberry-like structures can be easily found in the center of the heating area. As all these mulberry-like structures are arranged in no order at this moment, they definitely have no relationship with crystal. To further analyze the situations that affect the crystal forming, different power including 7% and 10 % power of the laser beam have been applied to other samples. But the results didn't change much until the cooling process has been changed.

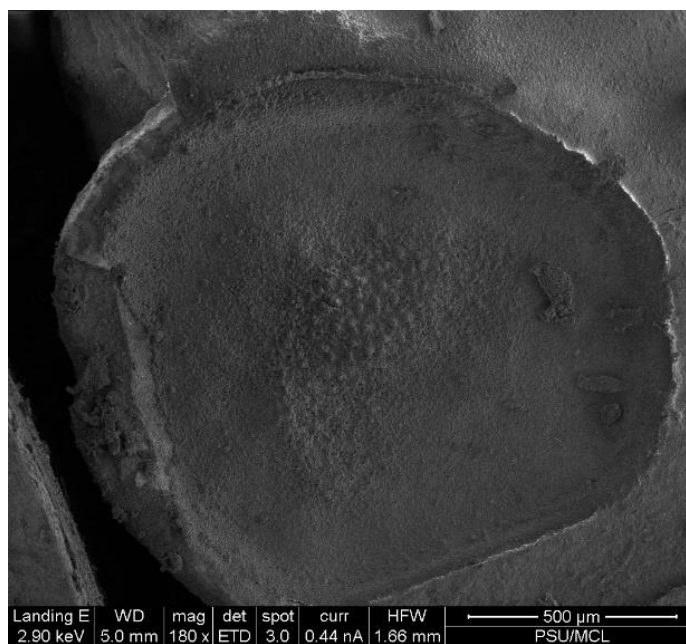


Figure 3-1. Sample heating two minutes with 5% power and cooling immediately after heating

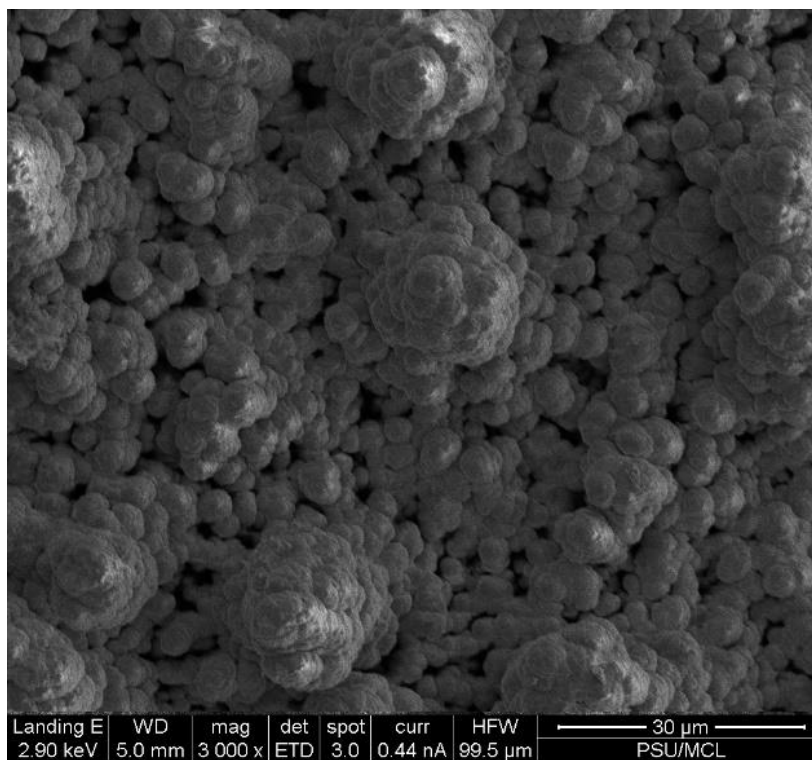


Figure 3-2. The central area of the sample

The following figure 4-1 presents the crystals appear near the heating hole area compared with the figure shown above. This is a sample heating for two minutes with 12% power and cooling slowly for another 2 minutes. From the figure 4-2, edges can be seen clearly which provides more supports for crystals. And the figure 4-3 presents the largest one, which has 50 micrometers' diameter. Figure 4-4 is the original powder on the surface. The particles without heating is much smaller than the crystal with cooling process. Therefore, the cooling process plays an important role in the growth of the crystal. The component of the crystal structures is analyzed by EDS and XRD.

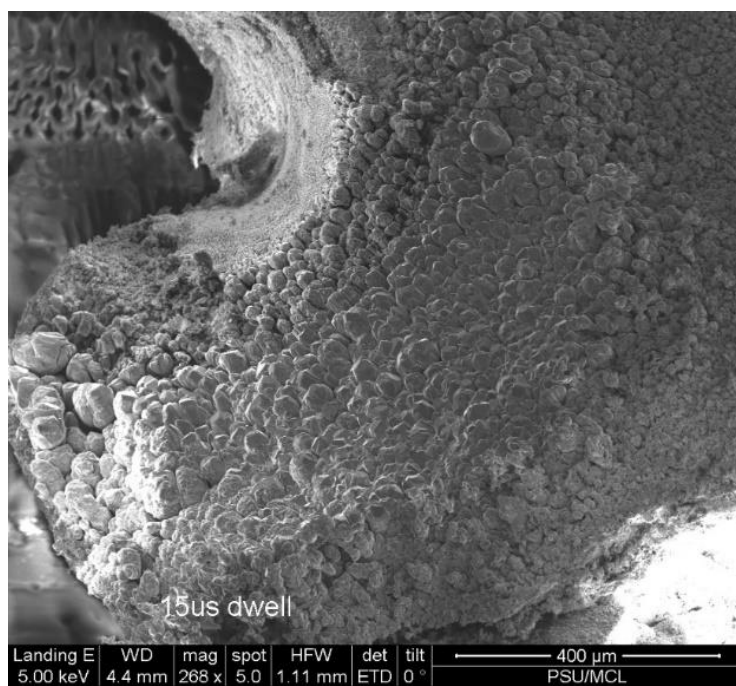


Figure 4-1. Sample heating for two minutes with 12% power and cooling slowly for another two minutes

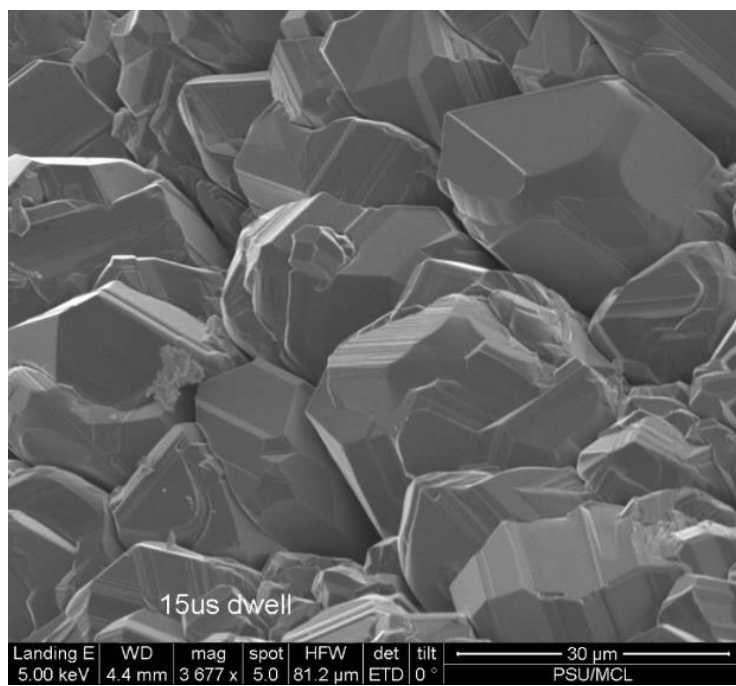


Figure 4-2. Crystals with clear edge

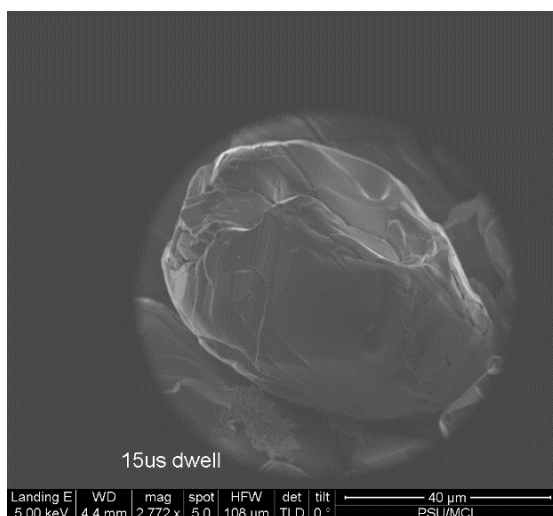


Figure 4-3. The largest crystal

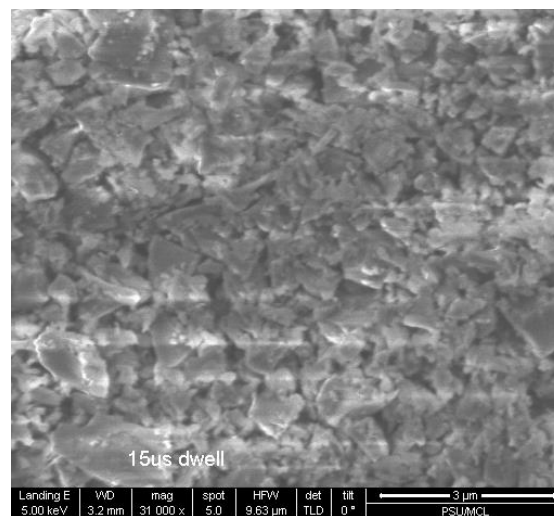


Figure 4-4. Original powder on surface

By repeating the experiments several times, another important result has been found that the crystal grows mostly in the middle layer of the samples and the cross section of the heating area. Due to the fact that all the samples are prepared without any adhesive, the samples can break into several pieces easily. In this research, samples usually split themselves after heating and the new “surface” is the layer where crystals grow. Another experiment with heating power of 10% for two minutes and cooling for two minutes has been made for further study. After the first cooling process, the sample was heated again with the same power and time but with a different cooling time of three minutes. This sample split itself into three layers and both layers appear crystal-like structures. And the third layer has a broadened range. This result shows that the cooling process provides time and energy for silicon carbide growth.

From the macro-perspective, the figure 5-2 is the middle layer split after heating. Unlike the origin surface shown on the top left corner of figure 5-1, off-white color, dark green region and yellow-white sugar-like structures appear around the heating hole. The pure silicon carbide

should be completely transparent. 3C-SiC has the color of yellow and α -SiC has the color of green to dark green. Therefore, these yellow-white structures indicate that the 3C-SiC grows more and larger than the other types and appears near the heating area. The figure 5-4 is the microstructure of the yellow-white part



Figure 5-1. Surface layer

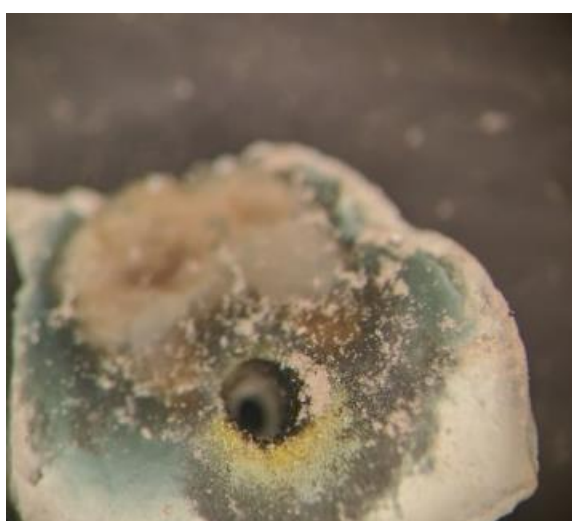


Figure 5-2. Middle layer

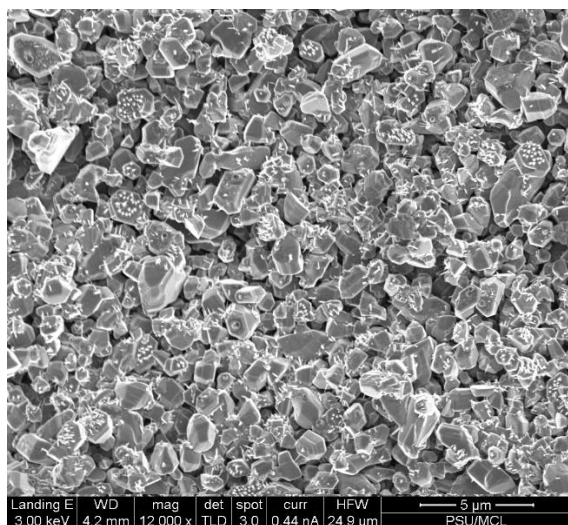


Figure 5-3. Microstructure of the surface

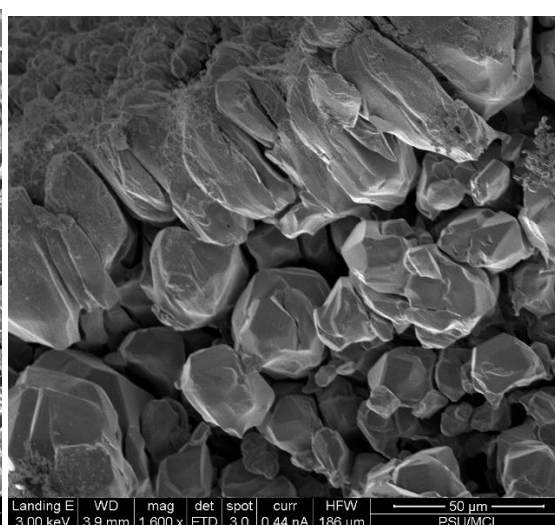


Figure 5-4. Microstructure of the middle layer

Besides the inner layer surface, another place to find crystal is the cross section of the heating area. Unlike the cohesion-less structures, a pycnomorphic hemisphere has been formed around the heating point. The figure 6-1 shown below presents the vertical view of the cross section of the heating hole. Although there is not any large crystal, the powders are connected to each other to forming bands which strengthen the hardness of this hemisphere. The figure 6-2 shown below is the side view of the cross section. These bonds start to generate crystals. By comparing these two figures, we can find that the bonds forming process is the initial step of growing crystals.

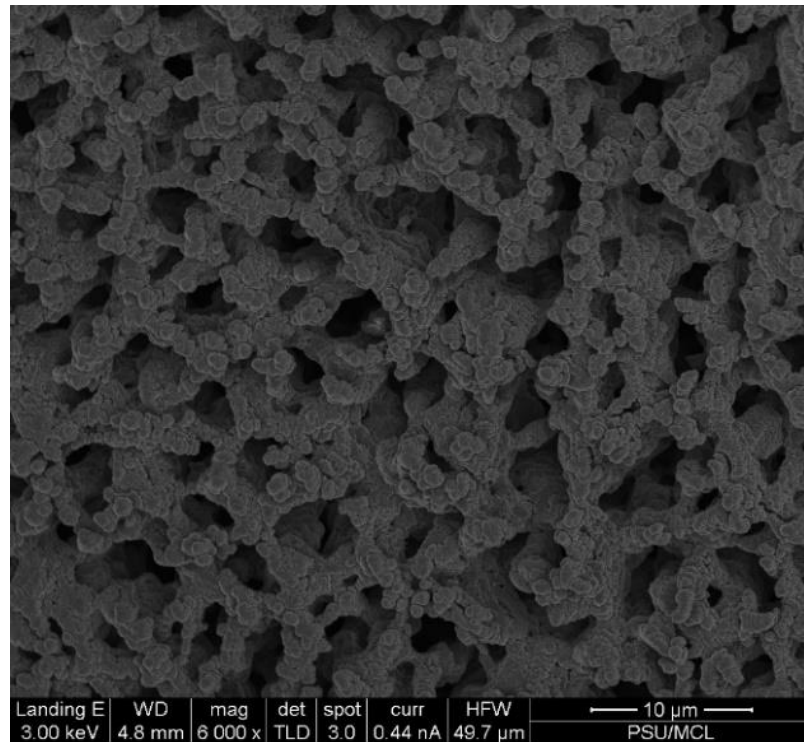


Figure 6-1. The vertical view of the cross section of the heating hole

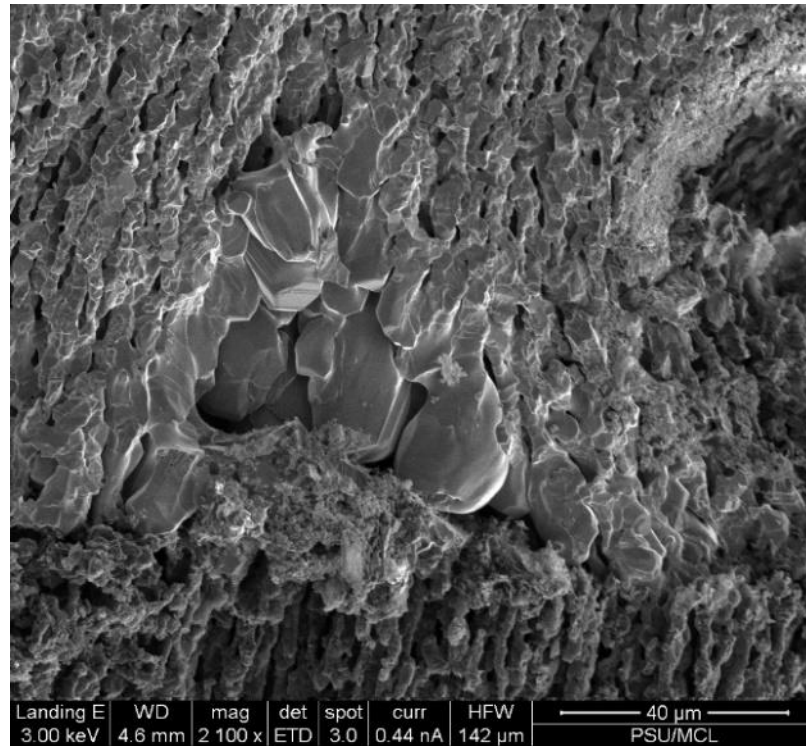


Figure 6-2. The side view of the cross section

Energy dispersive spectroscopy results and discussion

The figure 6 presents the elements species and the weight percentage of the crystal area. The most two elements are silicon and carbon with the weight percentage ratio nearly to 7 to 3. This weight ratio fit the silicon carbide crystal's compounds. Silicon has a standard atomic weight of 28.084 and carbon has a standard atomic weight of 12.096. (Meija *et al.* 2016) With the number ratio of 1:1, the weight ratio of silicon and carbon in silicon carbide is almost 7 to 3. The weight ratio is a proof of silicon carbide crystal. The polymorphism of silicon carbide is analyzed by X-ray diffraction

As all the samples storage in open air, oxidizing reactions are acceptable in this research.

Moreover, the calcium is probably caused by the previous samples characterized by the same energy dispersive spectroscopy. So, oxygen and calcium can be ignored.

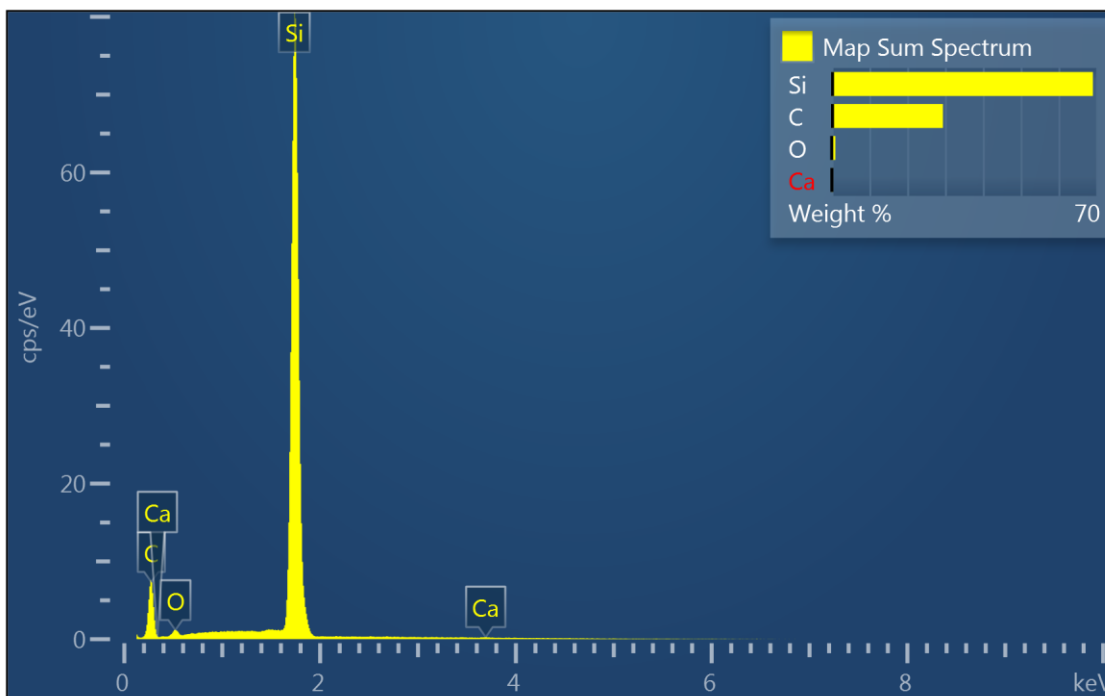


Figure 7. The energy dispersive spectroscopy result

X-ray diffraction results and discussion

The figure 7 is generated by software JADE and the data is collected by the PANalytical Empryeon with the X-ray wavelength of 1.54059\AA . From the figure 7, some peaks are located at 35.6123° , 41.44224° and 59.92998° . These three peaks fit the cubic phase 3C-SiC's (111), (200) and (220) lattice planes. Based on these data, the lattice constant is calculated by JADE to be 4.3589\AA which is close enough to 4.3596\AA (Taylor and Jones, 1960). The peak at 35.6123° is

extremely high and the peak at 59.92998° follows behind. So the crystal is mainly growing along the (111) direction with a high crystallinity.

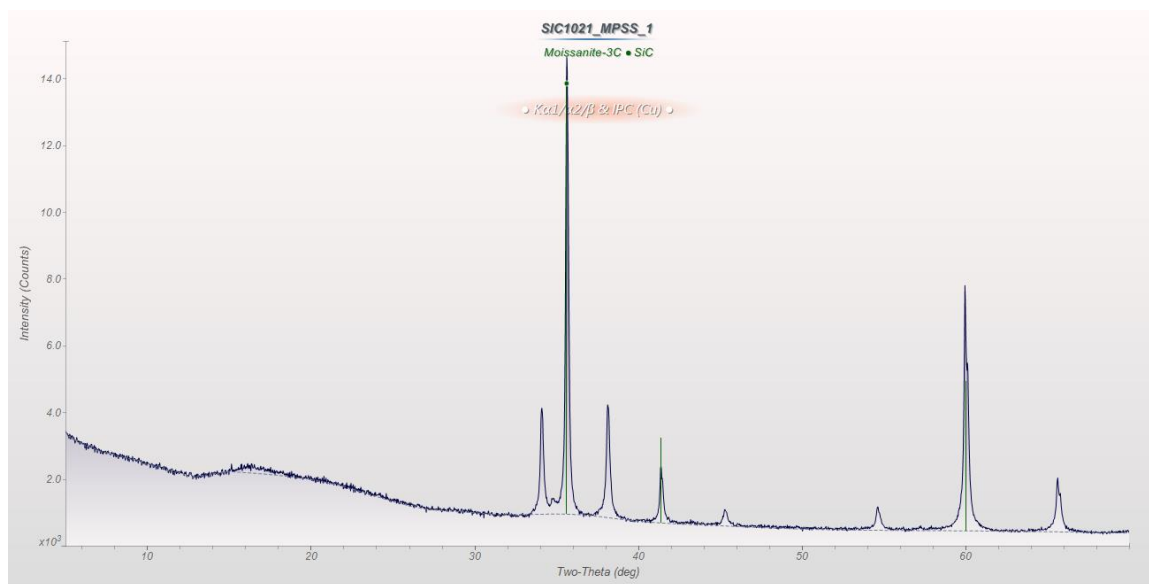


Figure 8. The X-ray diffraction result

Chapter 4

Conclusion

High temperature laser heating method provides us a new synthesis to grow silicon carbide crystals. It takes less time and cost less money to produce relatively large silicon carbide crystals. With the help of SEM, EDS and XRD, the final products can be determined to be silicon carbide crystal and mostly the 3C-SiC crystals. By changing the cooling process, we found that the cooling time plays an important role in crystal growth. Without enough cooling time, crystal structure won't form. And the repeated experiments present that the most crystals appear mainly in the middle layer of the samples instead of the heating surface. The initial step of forming crystal is to grow connected structures which has an improved hardness. And then the connected structures will fuse to grow large crystal structures. The peaks from XRD result give the proof of β phase silicon carbide and they are mainly growing along the (111) direction. The largest crystal in this research has a diameter of 50 micrometers which is hundreds bigger than the original powder size.

References

- Casady, J. B., and R. W. Johnson. Status of Silicon Carbide (SiC) as a Wide-Bandgap Semiconductor for High-Temperature Applications: A Review. vol. 39, Elsevier Ltd, 1996, doi:10.1016/0038-1101(96)00045-7
- Keilmann, F., T. Taubner, and R. Hillenbrand. "Phonon-Enhanced Light-Matter Interaction at the Nanometre Scale." *Nature*, vol. 418, no. 6894, 2002, pp. 159-162, doi:10.1038/nature00899.
- Greffet, Jean-Jacques, et al. "Coherent Emission of Light by Thermal Sources." *Nature*, vol. 416, no. 6876, 2002, pp. 61-64, doi:10.1038/416061a.
- Cheung, Rebecca. *Silicon Carbide Microelectromechanical Systems for Harsh Environments*. Imperial College Press, Hackensack, NJ; London, 2006.
- Muranaka, Takahiro, et al. "Superconductivity in Carrier-Doped Silicon Carbide." *Science and Technology of Advanced Materials*, vol. 9, no. 4, 2008, pp. 044204, doi:10.1088/1468-6996/9/4/044204
- Scace, R. I., and G. A. Slack. "Solubility of Carbon in Silicon and Germanium." *The Journal of Chemical Physics*, vol. 30, no. 6, 1959, pp. 1551-1555, doi:10.1063/1.1730236.
- Ruddy, F. H., et al. "Development of a Silicon Carbide Radiation Detector." *IEEE Transactions on Nuclear Science*, vol. 45, no. 3, 1998, pp. 536-541, doi:10.1109/23.682444.
- Ilyakhinskii, IA, et al. "Acoustic Nondestructive Testing of Silicon Carbide/Graphite Composite." *Atomic Energy*, vol. 119, no. 6, 2016, pp. 414-418, doi:10.1007/s10512-016-0083-1.

Kruangam, Dusit, et al. "Visible-Light Injection-Electroluminescent a-SiC/p-i-n Diode." *Japanese Journal of Applied Physics*, vol. 24, no. Part 2, No. 10, 1985, pp. L806-L808, doi:10.1143/JJAP.24.L806.

Rastegaev, V. P., et al. "Features of SiC Single-Crystals Grown in Vacuum using the LETI Method." *Materials Science & Engineering B*, vol. 61, 1999, pp. 77-81, doi:10.1016/S0921-5107(98)00449-8.

Weaver, Samuel C., and Richard D. Nixdorf. "Method for the preparation of silicon carbide platelets." U.S. Patent No. 4,906,324. 6 Mar. 1990.

Nadkarni, Sadashiv K., and Mukesh K. Jain. "Process for producing silicon carbide platelets and the platelets so produced." U.S. Patent No. 5,080,879. 14 Jan. 1992.

Parent, Luc. "Process for producing silicon carbide platelets." U.S. Patent No. 5,258,170. 2 Nov. 1993.

Meija, Juris, et al. "Atomic Weights of the Elements 2013 (IUPAC Technical Report)." *Pure and Applied Chemistry*, vol. 88, no. 3, 2016, pp. 265-291, doi:10.1515/pac-2015-0305.

Taylor, A., Jones, R.M. "Silicon Carbide - A High Temperature Semiconductor", Eds. O'Connor, J.R., Smiltens, J., Pergamon Press, Oxford, London, New York, Paris 1960, 147.

Appendix A**Tables****Table 1. Prepared samples' weight.**

Number	Weight (g)	Number	Weight (g)
1	0.7001	11	0.6987
2	0.7006	12	0.7035
3	0.6985	13	0.7003
4	0.7013	14	0.7004
5	0.6989	15	0.6994
6	0.7011	16	0.7021
7	0.7012	17	0.6987
8	0.7020	18	0.6998
9	0.7003	19	0.7018
10	0.7015	20	0.7006

Table 2. The conditions of experiments.

Settings	Value
Laser power	20-30W
Focusing spot size	1 mm^2
Exposure time	2-3min
Cooling time	2min

Appendix B

Figures

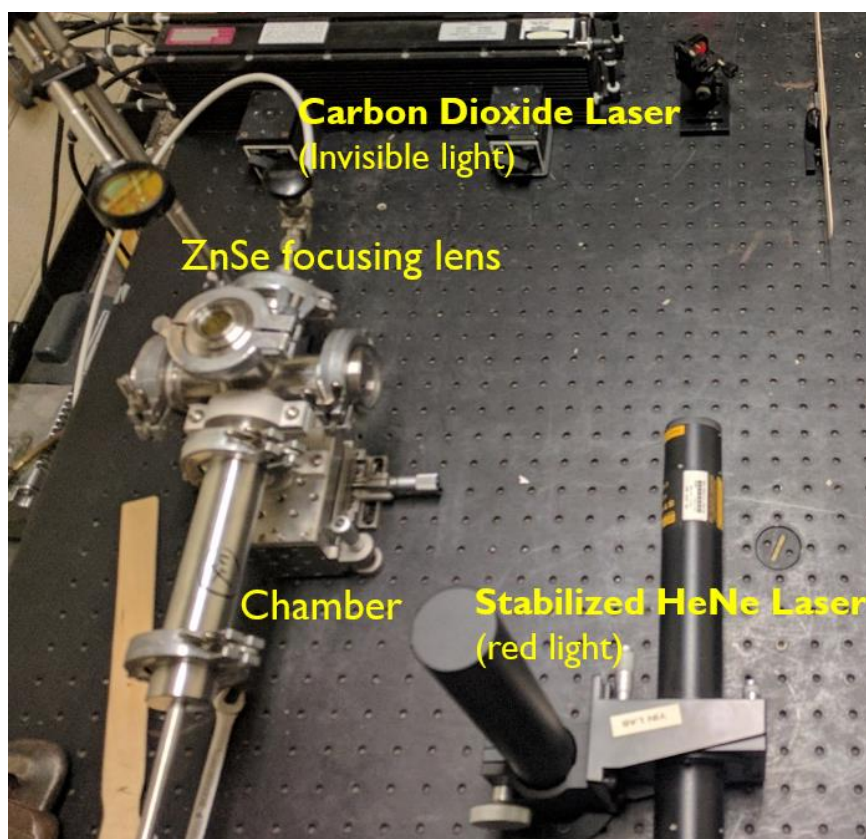


Figure 1. The setup of the experiment equipment.

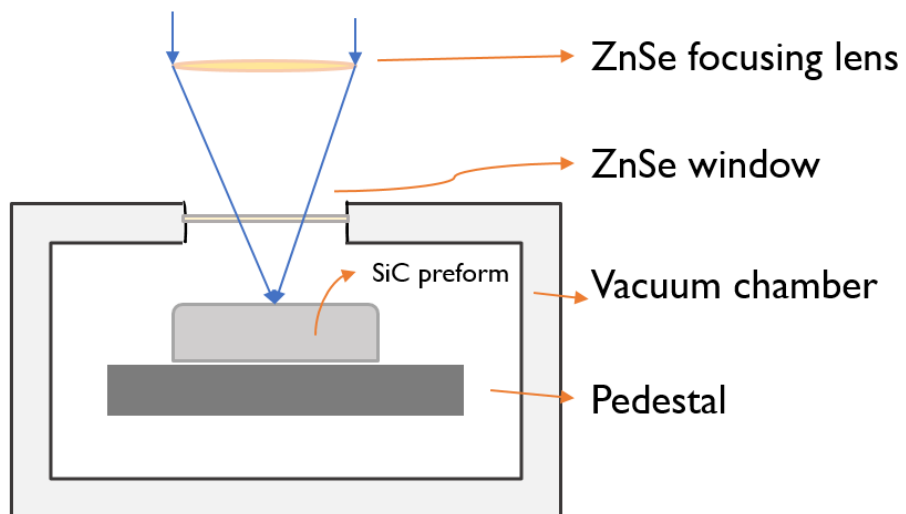


Figure 2. The enlarged view of the chamber.

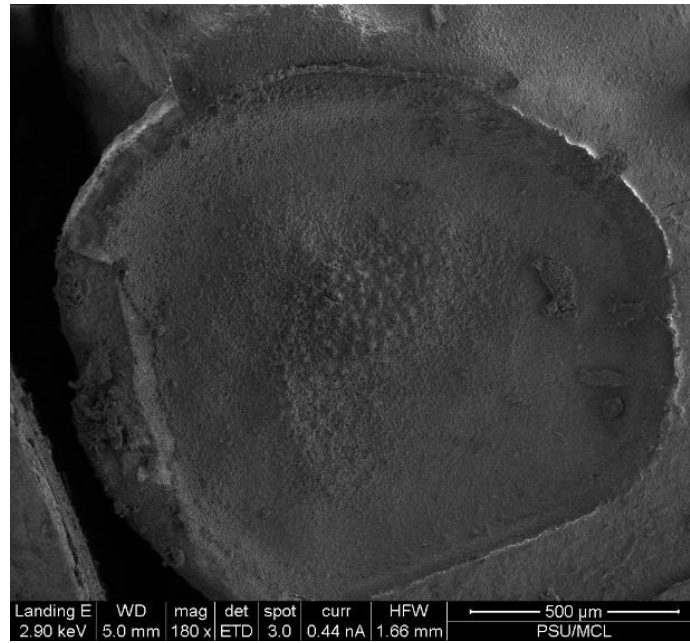


Figure 3-1. Sample heating two minutes with 5% power and cooling immediately after heating.

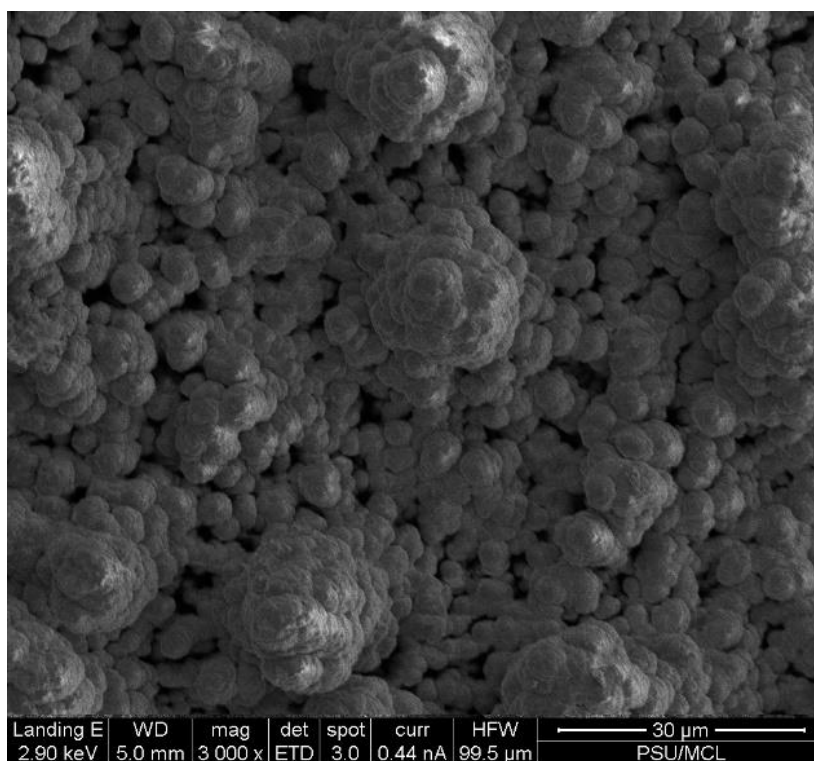


Figure 3-2. The central area of the sample

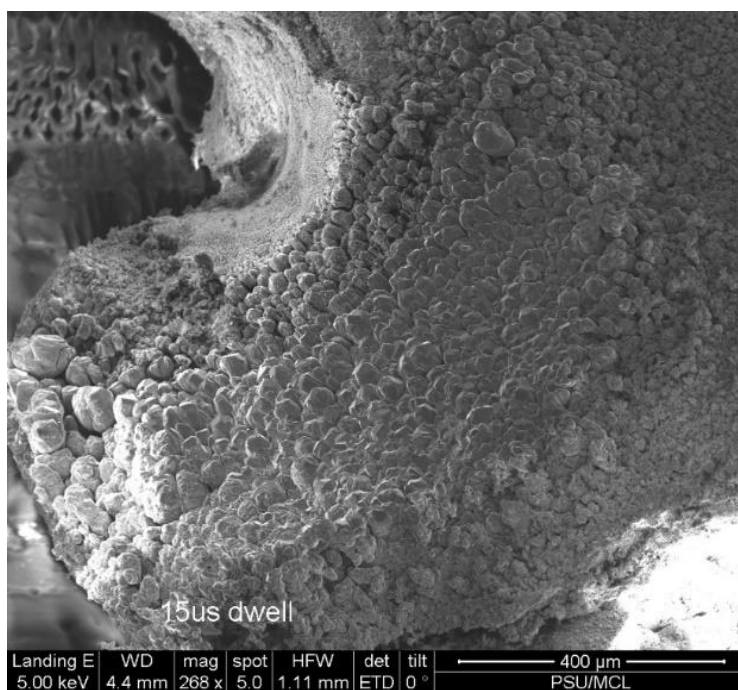


Figure 4-1. Sample heating for two minutes with 12% power and cooling slowly for another two minutes

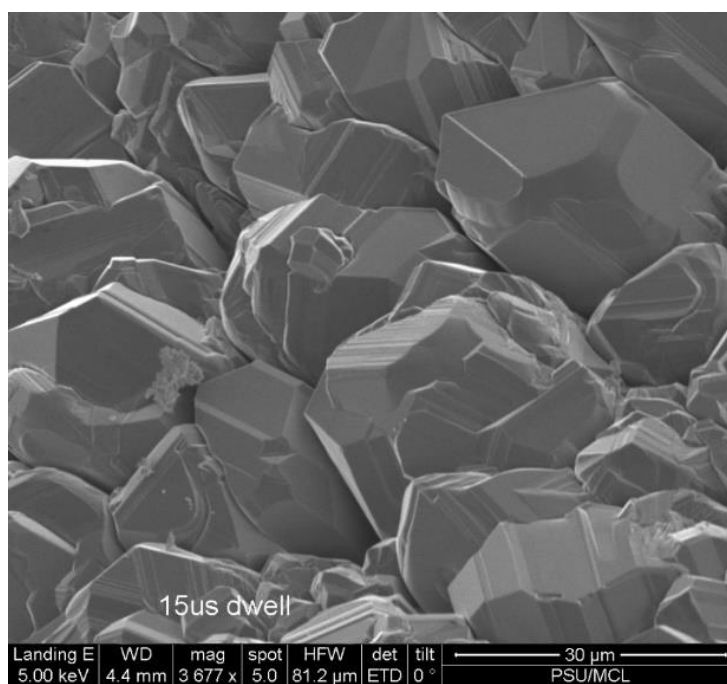


Figure 4-2. Crystals with clear edges

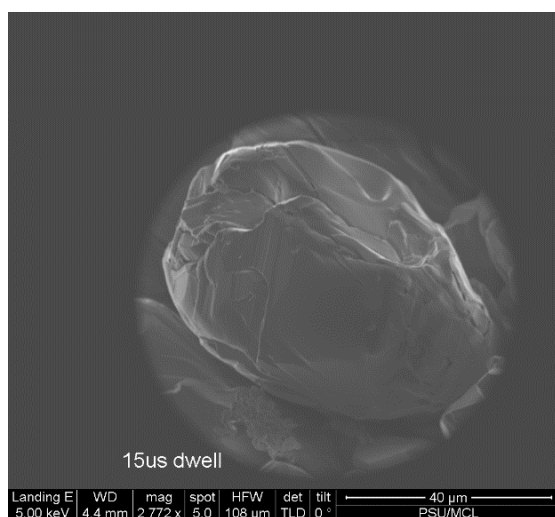


Figure 4-3. The largest crystal

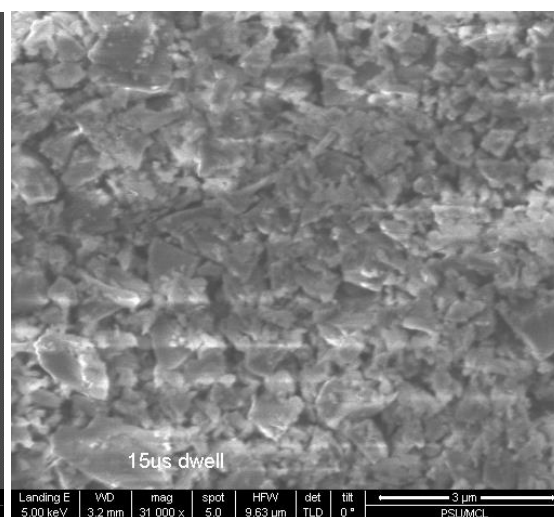


Figure 4-4. Original powder on surface

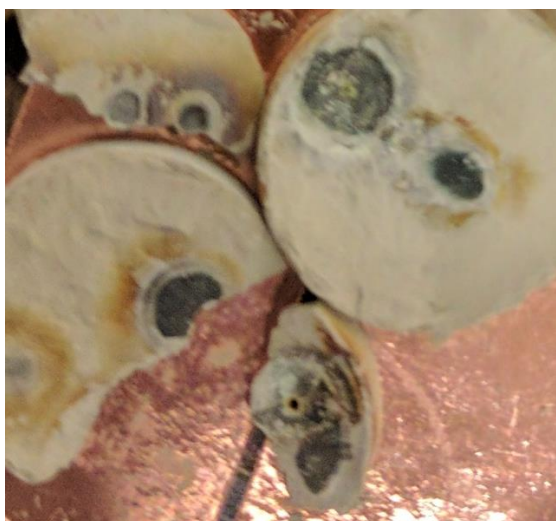


Figure 5-1. Surface layer

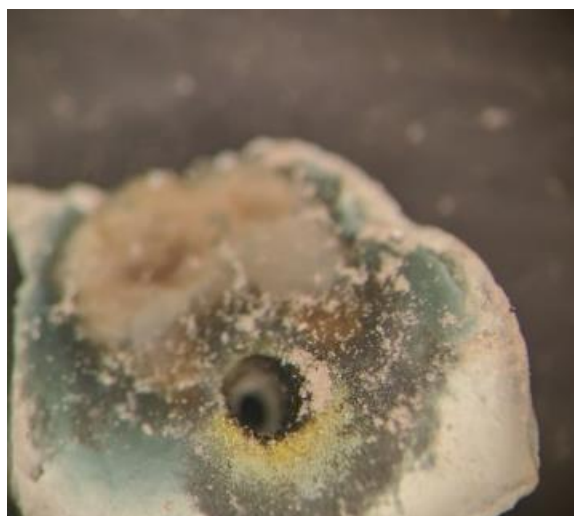


Figure 5-2. Middle layer after heating

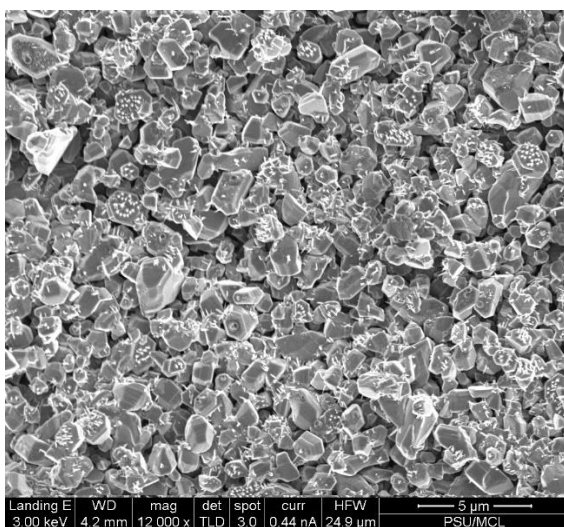


Figure 5-3. Microstructures of surface

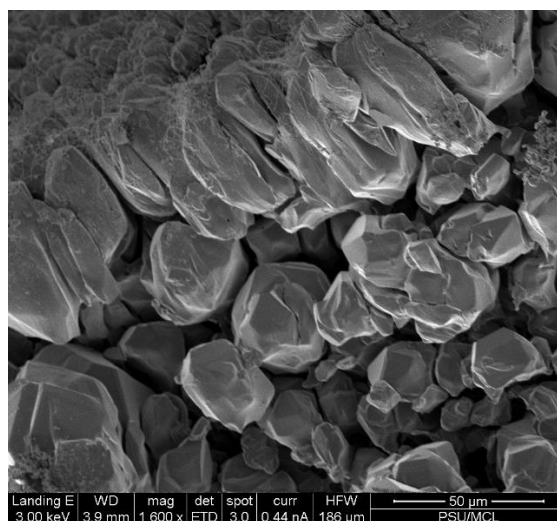


Figure 5-4. Microstructures of middle layer

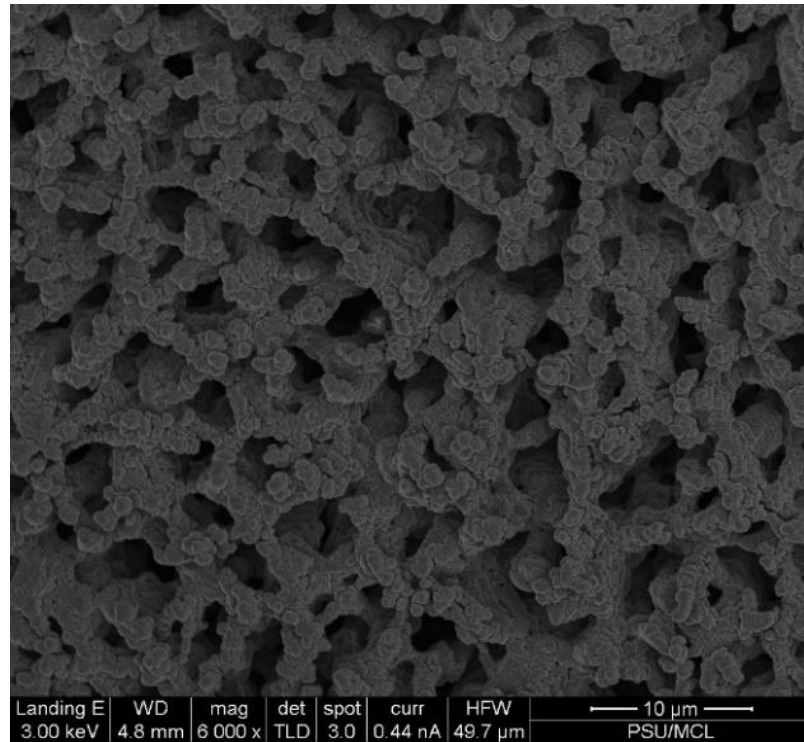


Figure 6-1. The vertical view of the cross section of the heating hole

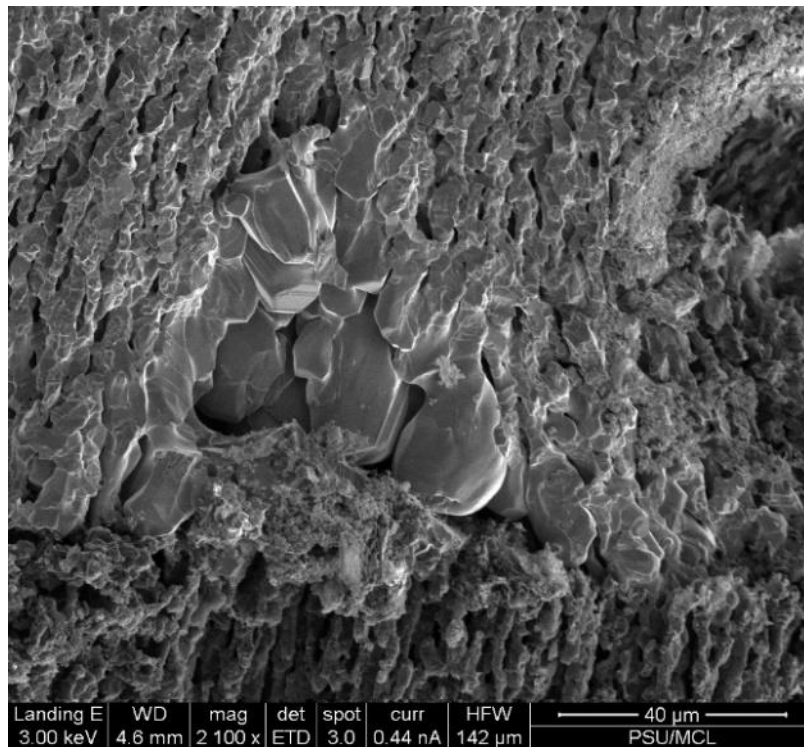


Figure 6-2. The side view of the cross section

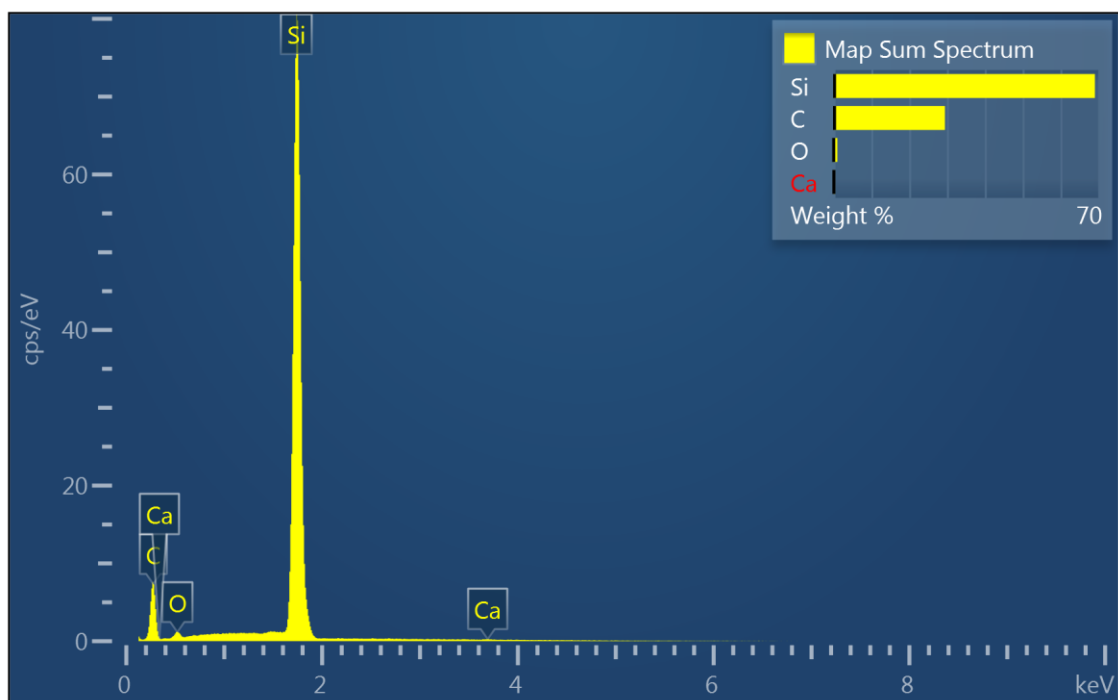


Figure 7. The energy dispersive spectroscopy result

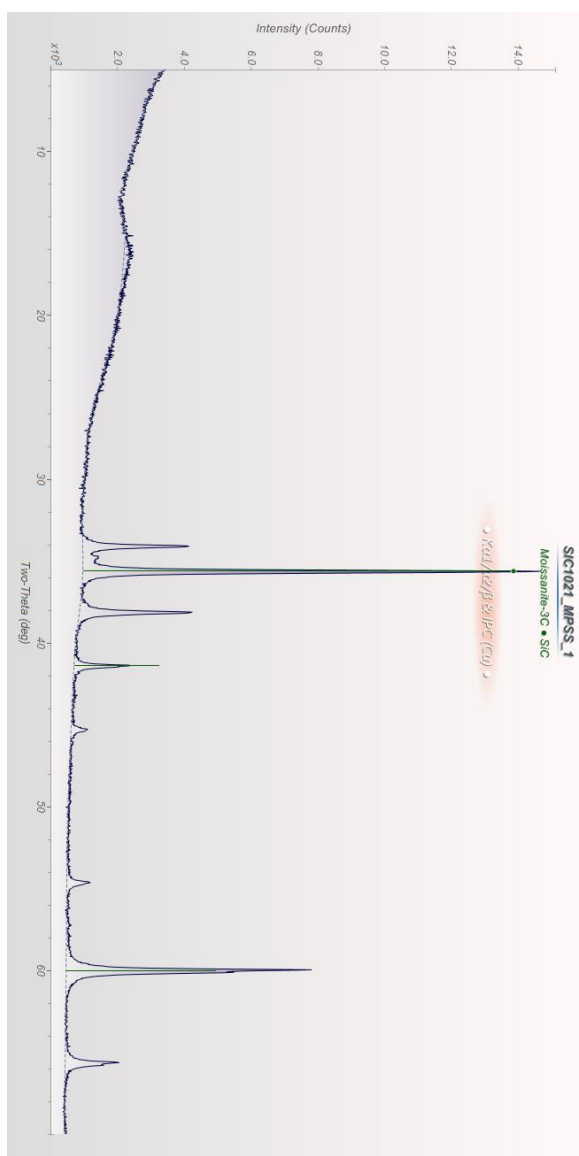


Figure 8. The X-ray diffraction result